Supplementary Information

Metal elements-fusion peptide heterostructured nanocoating bestows polyetheretherketone implants with robust anti-bacteria and *in vivo* osseointegration

Hao Yang,[a] Haiyang Ding,[a] Yu Tian,[a] Chao Wu,[f] Yanbai Chen,[a] Hongxing Shi,[a] Yau Kei Chan,[e] Yi Deng,[abc] Li Liao*[a] and Shuangquan Lai*[ad]

[a] *School of Chemical Engineering, Sichuan University, Chengdu 610065, China.*

[b] *State Key Laboratory of Polymer Materials Engineering, Sichuan University, Chengdu 610065, China.*

[c] *Department of Mechanical Engineering, The University of Hong Kong, Hong Kong, China.*

[d] *Zhuhai People's Hospital (Zhuhai Clinical Medical College of Jinan University), Zhuhai, Guangdong 519000, China.*

[e] *Department of Ophthalmology, The University of Hong Kong, Hong Kong 999077, China.*

[f] *Department of Orthopedics, Institute of Digital Medicine, Zigong Academy of Big Data for Medical Science and Artificial Intelligence, Zigong Fourth People's Hospital, Zigong, China*

* Corresponding authors at: School of Chemical Engineering, Sichuan University, Chengdu 610065, China.

E-mail addresses: liaolis@scu.edu.cn (Li Liao,) shuangquanlai@scu.edu.cn (Shuangquan Lai)

Captions of Figures

Supplemental Materials and Methods

Table S1. The primer sequences of Runx2, ALP, COL1α1, OCN, VEGF, HIF-1α, and bFGF.

Table S2. Quantitative analysis of micro-CT data including BV/TV, Tb.Th, Tb.N, and Tb.Sp at 4 weeks.

Table S3. Quantitative analysis of micro-CT data including BV/TV, Tb.Th, Tb.N, and Tb.Sp at 8 weeks.

Table S4. The maximum push-out forces of the implants at 8 weeks.

Fig. S1. EDS images of (a) SP, (b) SP-FMS, (c) SP-pFP, (d) SP-FMS-pFP.

Fig. S2. The hemolysis test (a) digital photographs and (b) hemolysis ratio of SP, SP-FMS, SP-pFP, and SP-FMS-pFP.

Fig. S3. Effects of SP, SP-FMS, SP-pFP, and SP-FMS-pFP on blood coagulation: (a) APTT, (b) FIB, (c) PT and (d) TT.

Fig. S4. Construction of the rabbit femur implantation model.

Fig. S5. (a) Reconstructed micro-CT images and (b) X-ray images of rabbit femurs after implantation at 4 weeks and 8 weeks.

Fig. S6. (a) Load-displacement curves of the implants at 8 weeks.

Fig. S7. (a) The statistical analysis of the newly generated bone tissue in the toluidine blue-fuchsine staining images. (b) The statistical analysis of the calcified tissues labeled by calcein in the fluorescent staining images.

1. Supplemental Materials and Methods

1.1 Materials

PEEK (biomedical grade, processed into disks (Φ 8.5×2 mm)) was purchased from GEHR Plastic Inc. (Mannheim, German) and cleaned in acetone and ultrapure water with ultrasound assistance sequentially before utilized for material preparation. Ferric chloride ($FeCl_3$), magnesium chloride ($MgCl_2$), strontium chloride ($SrCl_2$), tris(hydroxymethyl)aminomethane (Tris), sodium bicarbonate ($NaHCO_3$), sodium hydroxide (NaOH), sulphuric acid (H_2SO_4), hydrochloric acid (HCl), ethanol, acetone were provided by Kelong Chemical Reagent Factory (Chengdu, China). Hydrochloride dopamine was obtained from Aladdin (Shanghai, China). Fusion peptide (KGQGFSYPYKAVFSTQKLTWQELYQLKYKGI) was acquired from ChinaPeptides Co., Ltd. (Shanghai, China).

1.2 Characterization

The microstructures of different samples (SP, SP-FMS, SP-pFP, and SP-FMS-pFP) were observed using SEM (JSM-7500F) and elemental analysis of samples were conducted by EDS (SDD-550) equipped on SEM machine. The surface compositions and chemical sate of the samples were determined by XPS (XSAM800). Wide-scan surveys were characterized, and subsequently high-resolution scans of the Fe 2p, Mg 1s, Sr 3d, and N 1s peaks were measured. The hydrophilicity of samples was investigated by utilizing a WCA tester (JC2000C1). The release behaviors of Fe^{3+}, Mg^{2+} and Sr^{2+} ions in the PBS solution were measured by ICP-AES (5100 SVDV).

1.3 *In Vitro* Hemocompatibility Testing

In vitro hemocompatibility assessment was performed by evaluating the blood coagulation and hemolysis indexes of rabbit blood (Yuduo Biotechnology Co., Shenzhen, China) in presence of different samples. Rabbit whole blood was first centrifuged (4000 rpm, 4 ^{o}C, 15 min) to remove blood cells. Subsequently, the obtained plasma was mixed with different

samples at 37 °C for 15 min. Finally, a semi-automatic coagulation analysis meter (PUN-2048B, Perlong) was used to measure the PT, TT, FIB, and APTT. In hemolysis testing experiment, the rabbit blood was first mixed with different samples (normal saline: negative control group, ultrapure water: positive control group) for 60 min at 37 °C, and then the OD value of the supernatant was measured (microplate reader at 545 nm). The hemolysis ratio of the samples was calculated by utilizing the following equation:

$$\text{Hemolysis Ratio (\%)} = [(OD_{sample} - OD_{negative}) / (OD_{positive} - OD_{negative})] \times 100\%$$

where OD_{sample} represents the optical density value experimental group, $OD_{negative}$ and $OD_{positive}$ represent the optical density value of negative and positive control groups, respectively.

1.4 *In vitro* cell experiments

1.4.1 Micro-CT observation. The collected rabbit femoral bones with implants were analyzed by micro-CT (SCANCO VivaCT80) using the same parameters (voltage: 70 kVp, isotropic voxel size: 15 μm, integration time: 300 ms), and 3D models were constructed. Moreover, the BV/TV, Tb.Sp, Tb.Th, and Tb.N were also computed.

1.4.2 Biomechanical measurement. The biomechanical measurement was performed using push-out method, which was considered as the best way to evaluate the osteointegration capability of the implant. Push-out tests were carried out using an electronic universal tester (Instron 8874, Norwood). Briefly, to record the load-displacement curve, an axial compression load (velocity: 5 mm/min) was applied to the implant, recording the curves until the bone and implant boundary was completely disrupted. After completing the biomechanical property measurement, the implants that isolated from the pushed-out test bone were utilized to SEM and EDS mapping characterizations to observe the bone ingrowth around the implants.

1.4.3 Histological evaluation. The obtain bones were dehydrated utilizing ethanol solutions with different concentration gradients (70, 80, 90, 100%), and sequentially embedded in poly(methyl methacrylate) (PMMA) resin. Sections (80 μm in thickness) were vertically

sliced along the obtained implants using a microtome (RM2125, Leica). Afterwards, the obtained sections were stained by toluidine blue-fuchsine in order to detect the bone ingrowth situation on the implant. Furthermore, the calcified tissues were also labeled by calcein, and the fluorescence images of these sections were captured by CLSM.

2. Supplemental Tables and Figures

2.1 Supplemental Tables

Table S1. The primer sequences of Runx2, ALP, COL1α1, OCN, VEGF, HIF-1α, and bFGF.

Target Genes	Primer Sequences (F= forward, R= reverse)
RUNX2	F: 5'- CCGGGAATGATGAGAACTA-3' R: 5'- GGACCGTCCACTGTCACTTT-3'
ALP	F: 5'- GCTGATCATTCCCACGTTTT-3' R: 5'- CTGGGCCTGGTAGTTGTTGT-3'
COL1α1	F: 5'- AGAGCATGACCGATGGATT-3' R: 5'- TGAGCTCGATCTCGTTGGATR-3'
OCN	F: 5'- GAACAGACTCCGGCGCTA-3' R: 5'- AGGGAGGATCAAGTCCCG-3'
VEGF	F: 5'- ACCTCATGCTGATACCGGGTCC-3' R: 5'- CCGGGGCGTGGAGTACCTGT-3'
HIF-1α	F: 5'- CGTCGCTTCGGCCAGTGTGT-3' R: 5'- TCCAGAGGTGGGGGTGCGAG-3'
bFGF	F: 5'- ACCCTCACATCAAGCTACAAC-3' R: 5'- AAAAGAAACACTCATCCGTAA-3'

Table S2. Quantitative analysis of micro-CT data including BV/TV, Tb.Th, Tb.N, and Tb.Sp at 4 weeks.

	SP	**SP-FMS**	**SP-pFP**	**SP-FMS-pFP**
BV/TV (%)	7.29190	7.45245	1.67412	9.22714
Tb.Th (mm)	0.12812	0.09457	0.05861	0.09730
Tb.N (mm^{-1})	0.56913	0.78800	0.28562	0.94828
Tb.Sp (mm)	1.68817	1.58679	1.86684	1.60592

Table S3. Quantitative analysis of micro-CT data including BV/TV, Tb.Th, Tb.N, and Tb.Sp at 8 weeks.

	SP	**SP-FMS**	**SP-pFP**	**SP-FMS-pFP**
BV/TV (%)	8.84961	5.77006	8.08435	10.56968
Tb.Th (mm)	0.09691	0.08439	0.10530	0.10600
Tb.N (mm^{-1})	0.91321	0.68372	0.76776	0.99716
Tb.Sp (mm)	1.67220	1.76093	1.70292	1.59819

Table S4. The maximum push-out forces of the implants at 8 weeks.

	SP	**SP-FMS**	**SP-pFP**	**SP-FMS-pFP**
Fmax (N)	45.58273	98.80673	135.04602	208.30618

2.2 Supplemental Figure S1-S7

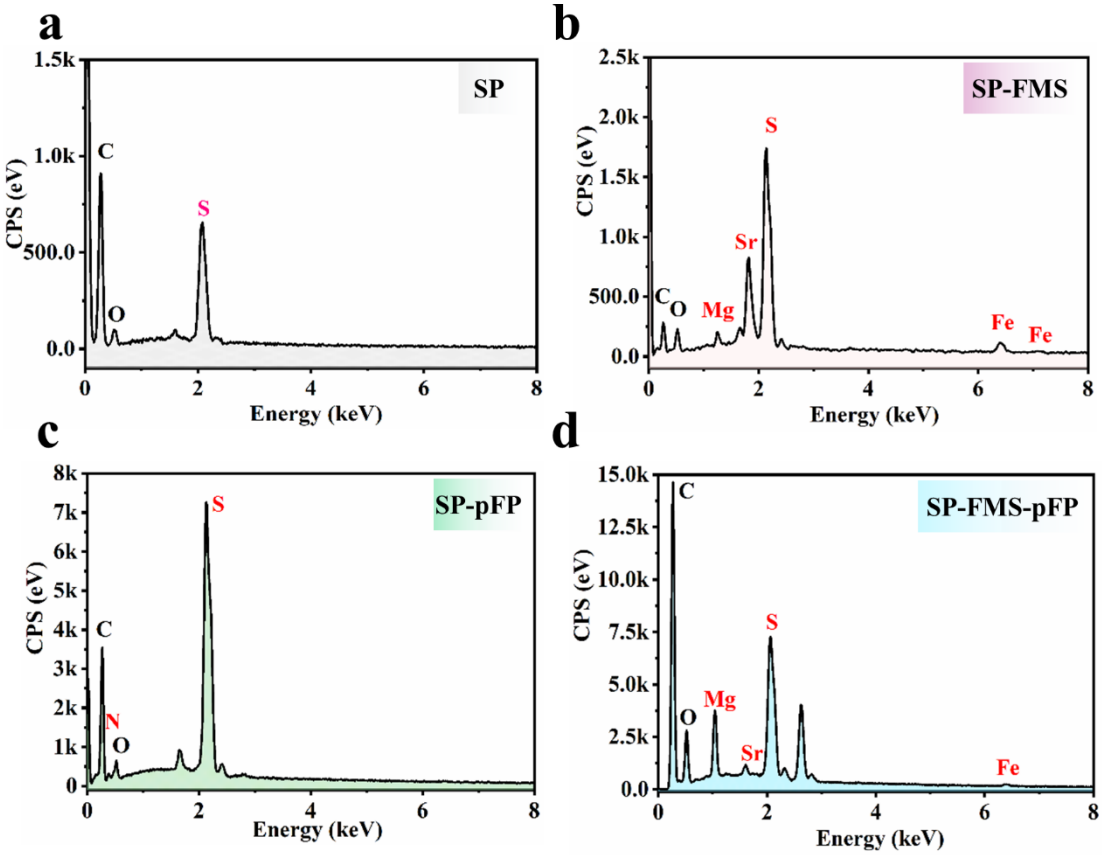

Fig. S1. EDS images of (a) SP, (b) SP-FMS, (c) SP-pFP, (d) SP-FMS-pFP.

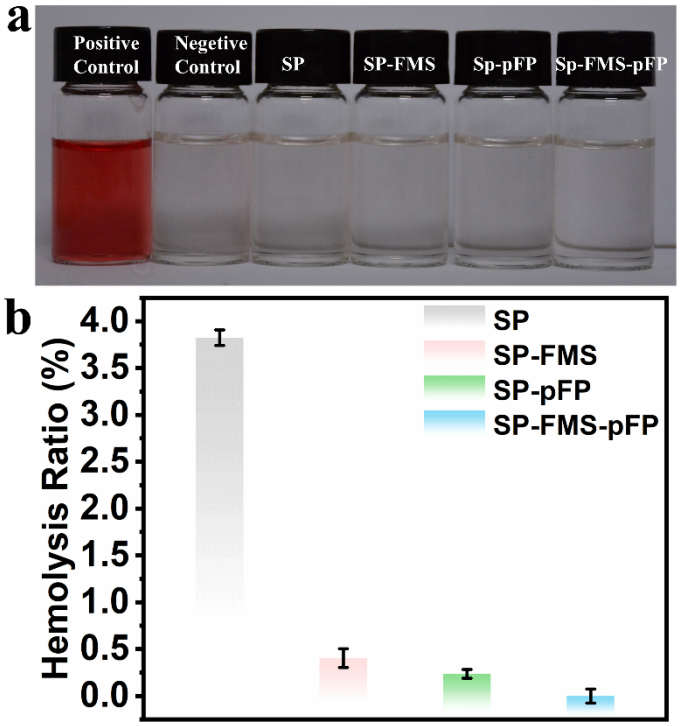

Fig. S2. The hemolysis test (a) digital photographs and (b) hemolysis ratio of SP, SP-FMS, SP-pFP, and SP-FMS-pFP.

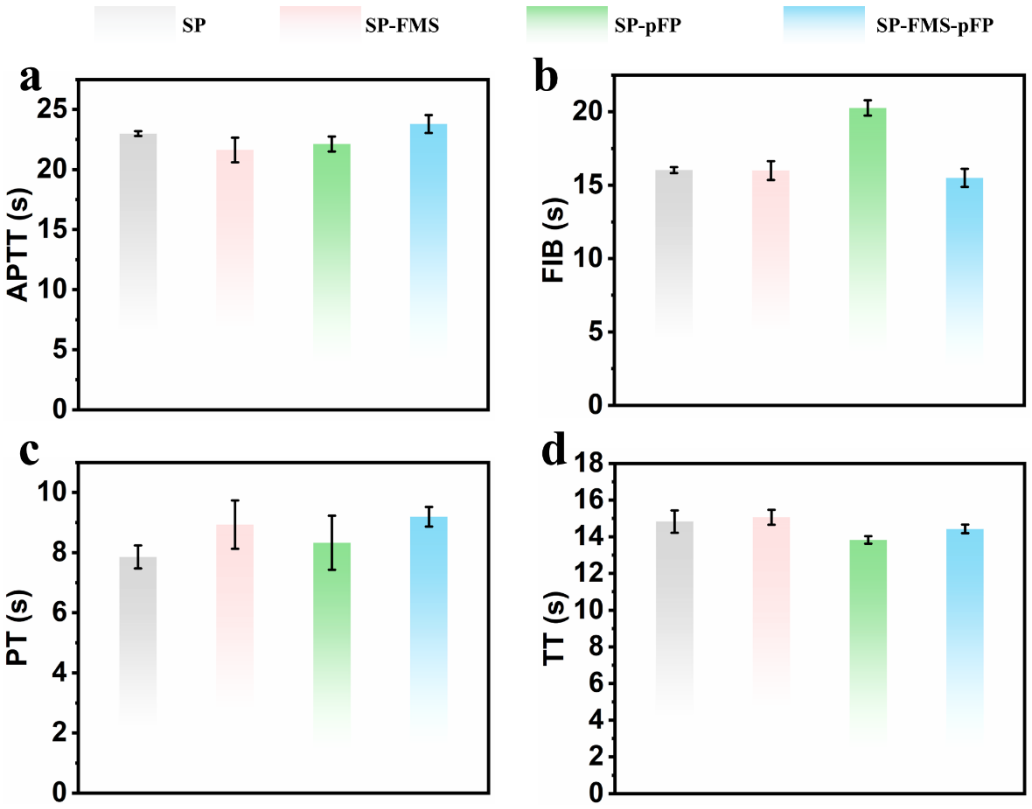

Fig. S3. Effects of SP, SP-FMS, SP-pFP, and SP-FMS-pFP on blood coagulation: (a) APTT, (b) FIB, (c) PT and (d) TT.

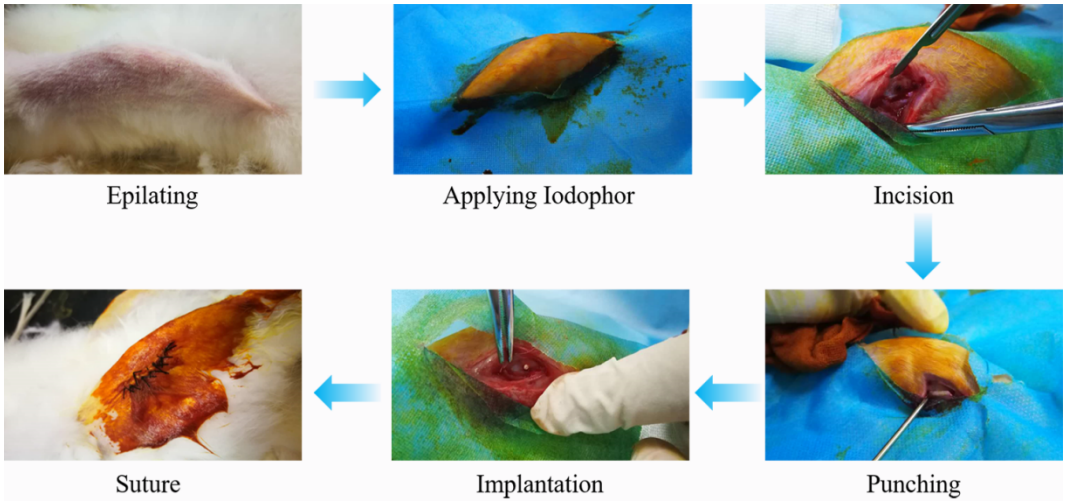

Fig. S4. Construction of the rabbit femur implantation model.

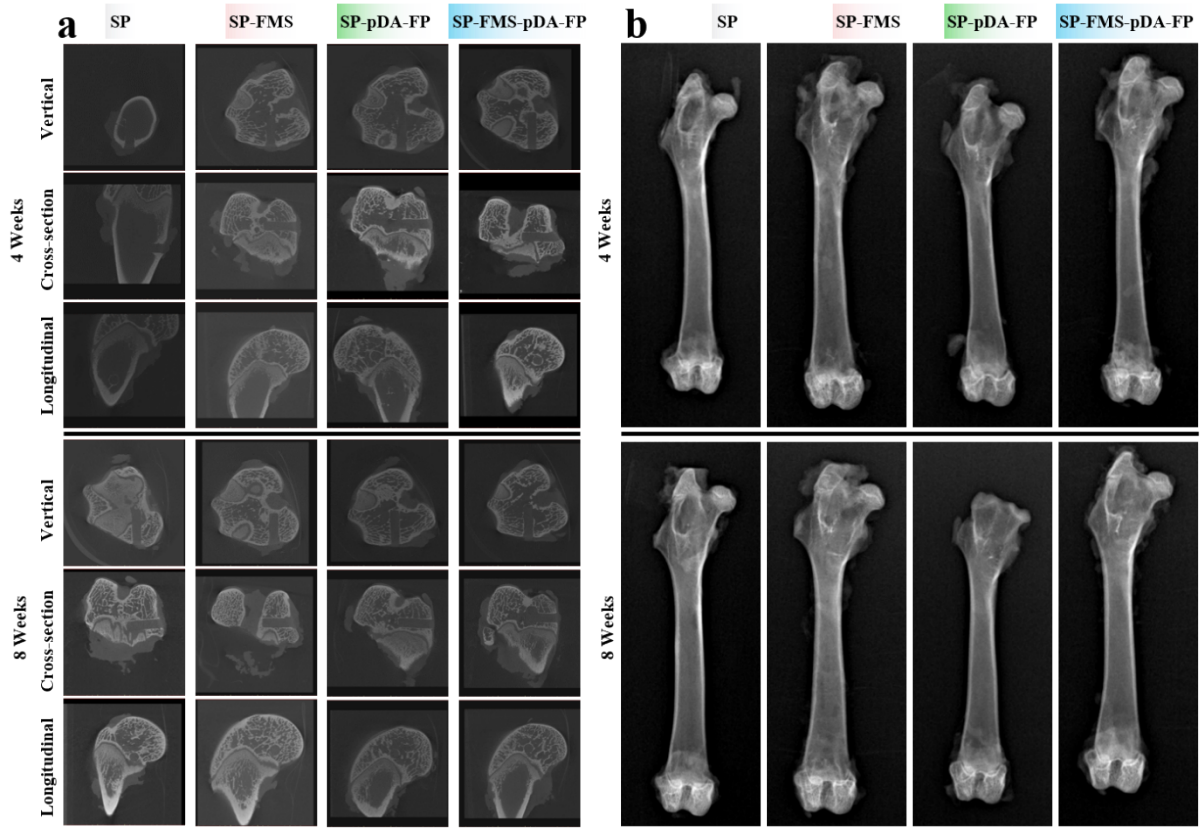

Fig. S5. (a) Reconstructed micro-CT images and (b) X-ray images of rabbit femurs after implantation at 4 weeks and 8 weeks.

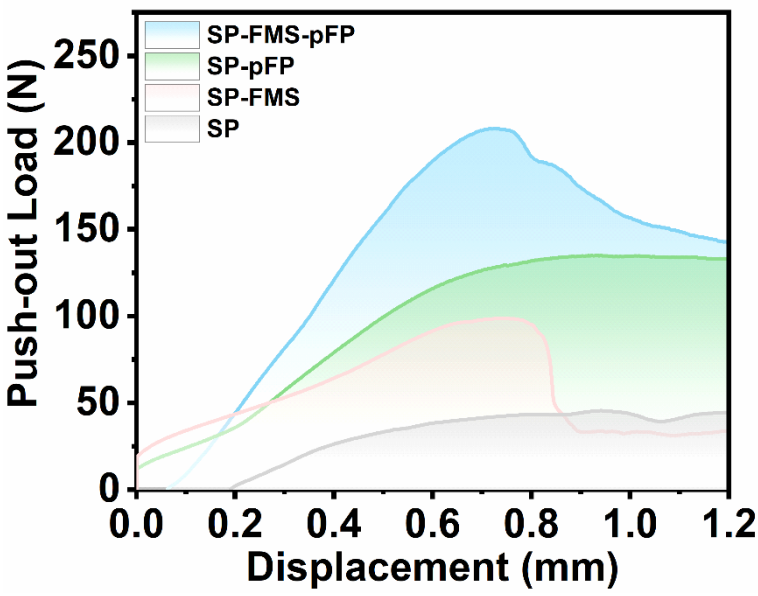

Fig. S6. (a) Load-displacement curves of the implants at 8 weeks.

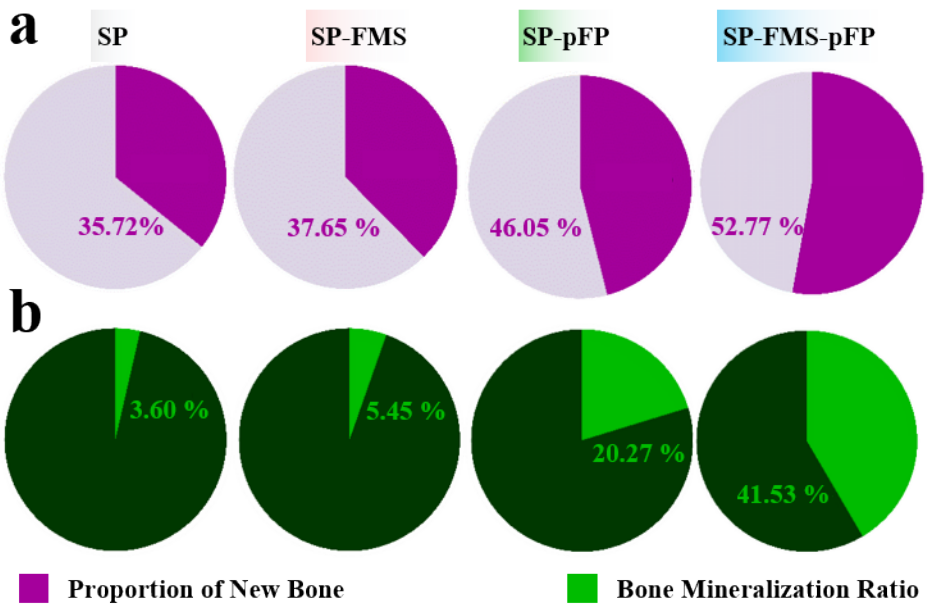

Fig. S7. (a) The statistical analysis of the newly generated bone tissue in the toluidine blue-fuchsine staining images. (b) The statistical analysis of the calcified tissues labeled by calcein in the fluorescent staining images.